N92-23293

GAMMA RADIATION SURVEY OF THE LDEF SPACECRAFT

G.W. Phillips, S.E. King, R.A. August, and J.C. Ritter
U.S. Naval Research Laboratory
Washington, DC 20375
Phone: 202/767/5692, Fax: 202/767-3709

J.H. Cutchin
Sachs/Freeman Associates
Landover, MD 20785
Phone: 202/767/5692, Fax: 202/767-3709

P.S. Haskins
University of Florida
Gainesville, FL 32609
Phone: 904/371-4778, Fax: 904/372-5042

J.E. McKisson, D.W. Ely, and A.G. Weisenberger
Institute for Space Science and Technology
Gainesville, FL 32609
Phone 904/371/4778, Fax: 904/372-5042

R.B. Piercey, and T. Dybler
Mississippi State University
Mississippi State, MS 39762
Phone: 601/325-2806, Fax: 601/325-8898

SUMMARY

The retrieval of the Long Duration Exposure Facility (LDEF) spacecraft in January 1990 after nearly six years in orbit offered a unique opportunity to study the long term buildup of induced radioactivity in the variety of materials on board. We conducted the first complete gamma-ray survey of a large spacecraft on LDEF shortly after its return to earth. A surprising observation was the large ^{7}Be activity which was seen primarily on the leading edge of the satellite, implying that it was picked up by LDEF in orbit. This is the first known evidence for accretion of a radioactive isotope onto an orbiting spacecraft. Other isotopes observed during the survey, the strongest being ^{22}Na, are all attributed to activation of spacecraft components. ^{7}Be is a spallation product of cosmic rays on nitrogen and oxygen in the upper atmosphere. However, the observed density is much greater than expected due to cosmic-ray production in situ. This implies transport of ^{7}Be from much lower altitudes up to the LDEF orbit.

INTRODUCTION

Spacecraft in orbit around the earth undergo continuous bombardment by high-energy cosmic rays and energetic trapped protons. This results in the build up of small but observable amounts of induced radioactivity, depending on the material and the exposure history. The return to earth of the Long Duration Exposure Facility (LDEF) after nearly six years in orbit provided a unique opportunity to study the activation of the variety of materials on board due to exposure to the space radiation environment. Shortly after landing, and prior to removal of the experimental trays, we conducted a complete survey to determine the distribution of induced gamma radiation about the spacecraft. These observations should be useful in predicting the activation of future long-duration spacecraft such as the space station, orbiting earth sensors, and astronomical observatories.

Radiation is also induced in the upper atmosphere by the interaction of cosmic rays and trapped protons with nuclei of carbon, nitrogen, and oxygen. One of the products of these interactions, ^{7}Be, was observed during the survey of LDEF on the leading edges of the spacecraft in quantities much larger than expected from the known production cross sections and the known flux of cosmic rays and trapped protons at the altitudes of the LDEF orbit. In this article, we will describe the radiation survey results and discuss possible production and transport mechanisms for the ^{7}Be.

THE LDEF SPACECRAFT

The LDEF spacecraft was launched by the Space Shuttle Challenger on 7 April 1984. It was retrieved in orbit by the Shuttle Columbia on 12 January 1990 and brought back to Earth on 20 January 1990. The spacecraft is a 12-sided cylindrical aluminum structure, 9.1 m long by 4.2 m diameter, with a total weight of about 9700 kg. Along the sides and on both ends were 86 trays containing a broad range of passive or low-powered experiments designed to study the space environment in low-earth orbit and to determine the effects of the environment on various materials, coatings, and spacecraft components. It was launched into a nearly circular orbit at an altitude of 480 km and an inclination of 28.5 degrees, where it was exposed continuously to cosmic rays, interplanetary dust and the residual atmosphere. In addition, the orbit took it through the South Atlantic Anomaly (SAA) exposing the spacecraft to energetic trapped protons and electrons. In the months prior to retrieval, the orbit was decaying rapidly and LDEF was down to an altitude of about 310 km when recovered by the shuttle.

The orientation of the spacecraft was gravity-gradient stabilized while in orbit so that its axis was aligned to the Earth's radius vector, with one end always pointed toward space and the other end toward Earth. Also, rotation about this axis was stabilized with respect to the orbital velocity so that the leading edge was always side number 9 (plus about 8 degrees). There were a number of duplicate experimental trays positioned around LDEF in order to get information about the differential flux of particles and micrometeoroids. The LDEF orbital velocity (7.8 km/s at retrieval) exceeded the average thermal velocity of the rarified atmosphere so that exposure to the atmosphere was primarily on the leading edge of the spacecraft.

GAMMA RAY SURVEY

After landing, LDEF was returned to Kennedy Space Center (KSC) for post-recovery examination. There the spacecraft was mounted on a stand so that it could be rotated about its axis for inspection. During this period, an array of high-purity germanium detectors from the Naval Research Laboratory (NRL) and single detectors from the Institute for Space Science and Technology (ISST), were used to conduct the first detailed gamma-ray survey of a large spacecraft after exposure in low-earth orbit. The residual gamma-ray emission depends both on the flux of high-energy particles to which LDEF was exposed and on the particular materials in each experimental tray. To observe the distribution of gamma-ray activity about the spacecraft, we set up the array with detectors facing each tray position along one side of LDEF. The single detectors were positioned at each end facing one of the experimental trays. The distance from the detectors to each tray was about 0.6 m. Background spectra were taken prior to the arrival of LDEF, and the detectors were calibrated in place using known gamma-ray sources.

So as not to interfere with activities during the day, gamma-ray spectra were accumulated overnight for a minimum of 12 hours along each side . Each night, LDEF was rotated so that a new side faced the array and new trays faced the detectors at each end. In this manner the entire spacecraft was surveyed over the period from 4 to 20 February 1990. During the disassembly period which followed, spectra were taken of selected experimental trays after they were removed from LDEF.

GAMMA RAY OBSERVATIONS

We expected to see gamma rays from the decay of isotopes produced by the long bombardment of energetic protons, neutrons, and heavier cosmic rays. Figure 1 shows the accumulated gamma-ray spectrum over the six trays along side 9, which was at the leading edge. The strongest peaks observed above background were from positron annihilation (511 keV), and from the decays of ^{7}Be (478 keV) and ^{22}Na (1274 keV). Weaker peaks were observed from the decays of ^{54}Mn, and ^{56,57,60}Co. The observed activities were primarily due to activation of the most common materials on the spacecraft, aluminum and stainless steel (iron, nickel, and cobalt.) The exception is the unexpectedly strong activity from ^{7}Be which is discussed below. During post-collection data analysis, spectra were analyzed for each detector and peak intensities were extracted using the computer program HYPERMET (ref. 1). Table I gives the observed isotope, its gamma-ray energy, halflife, and observed activity averaged over the LDEF spacecraft and decay-corrected to the landing date (ref. 2).

Distribution of Gamma Ray Activities

The strongest isotopic activities observed during the radiation survey were from ^{22}Na and ^{7}Be, both of which are produced by spallation from high-energy protons on aluminum, the material of the spacecraft body and experimental tray holders. At equilibrium, the activity from

^{7}Be was expected to be lower than 22Na in intensity by two orders of magnitude from the ratio of their spallation yields on aluminum. However, the 478 keV line from ^{7}Be was unexpectedly strong at some positions around the LDEF. After the survey was complete, a plot of count rate versus position around the spacecraft showed that the ^{7}Be activity at the leading edge was strongly enhanced compared to the trailing edge. Figure 2 shows the distribution of the average ^{22}Na and ^{7}Be activities for each row of LDEF corrected to date of retrieval.

In contrast to ^{7}Be, the ^{22}Na activity in figure 2 shows a small enhancement at the trailing edge, although there is some variation due to the distribution of aluminum and other activation material around the spacecraft. The trailing edge enhancement can be attributed to the asymmetry in the trapped proton flux in the SAA (ref. 3). This flux is strongly peaked from the westward direction, the trailing direction in orbit . Although many of the trapped protons are energetic enough to penetrate LDEF, they could produce the asymmetry seen in the ^{22}Na activation data. In figure 3, the distribution of the positron annihilation activity shows a similar trailing edge enhancement. Although statistics are poor, there also appears to be a trailing edge enhancement in ^{54}Mn and possibly in the Co activities.

Unlike all the other observed distributions, a strong leading edge enhancement for the ^{7}Be activity is evident in figure 2. The weak activity seen from the trailing edge can be wholly accounted for by penetration of gamma rays from the opposite side of the hollow spacecraft. This distribution of the ^{7}Be activity is not consistent with any known mechanism for activation of the spacecraft materials. It can only be explained by accretion of the isotope onto the leading surfaces of LDEF as it moved through the thin upper atmosphere in orbit.

The overlay in figure 2 gives a diagram of LDEF. Each experimental tray position around the cylinder is identified by row, numbered 1 through 12, and bay, lettered A through F. The view is toward the space end and the leading edge; the arrow vectors indicate the direction of the orbital velocity. Figure 4 shows a two dimensional mapping of the ^{7}Be and ^{22}Na activity. The mapping shows the data as it would appear after cutting the cylinder between rows 1 and 12 and unrolling it flat. The data for each tray position is plotted by row (running from 1 to 12) along the right axis and by bay (running from A to F) along the left axis. The leading and trailing edges in orbit are identified by the dashed lines in the figure. The ^{7}Be activity is shown to be distributed along the entire leading edge and not confined to a single tray.

The data in figure 4 tend to be somewhat higher in the middle compared to the edges of the spacecraft. This can be explained by gamma rays from adjacent trays penetrating the 3 mm lead collimators which surrounded the detectors. Similarly, the weak trailing edge activity for ^{7}Be can be explained by penetration of gamma rays from the opposite leading edge.

The absence of ^{7}Be activity on the trailing edge was demonstrated by measurements of gamma-ray spectra from individual experimental trays after they were removed from LDEF. Figure 5 shows a comparison of spectra from nearly identical trays from the leading and trailing edges, containing germanium plates covered with a thin foil designed to capture interplanetary dust particles. The ^{7}Be peak is indicated in the figure and appears only on the tray from the leading edge.

Further confirmation of the lack of ^{7}Be on the trailing edge of LDEF came from low-level activity measurements of aluminum plates and tray clamps by NASA/Marshall Space Flight Center (MSFC) (ref. 4), which showed ^{7}Be activity only on parts from the leading edge. In addition, they found that an acid etch of an aluminum plate from the leading edge removed most of the activity, demonstrating that most of the ^{7}Be is on the surface.

DENSITY OF ^{7}BE IN THE UPPER ATMOSPHERE

Assuming that the ^{7}Be was accreted onto the surface of LDEF in low-earth orbit, the question arises: how did it get there with such intensity? From the literature, we can estimate the ^{7}Be density at 310 km due to cosmic-ray production for comparison to our measurements. Using curves of cosmic-ray interaction rates derived from measurements during a period of high solar activity (ref. 5) and including interactions due to the trapped proton flux, we obtain an estimated ^{7}Be density of 5.4×10^{-5} atoms/m^3 in the upper atmosphere at 0° to 30° and 310 km due to production in situ (see the Appendix for details.) From our measurements we can derive a capture rate which gives a minimum ^{7}Be density in orbit of 0.10 ± 0.03 atoms/m^3. This exceeds the estimated in-situ production by a factor of 1800.

It is difficult to explain such a large enhancement in the ^{7}Be density. One possibility is the mixing of air from the poles where the production rate is higher than at lower latitudes, which are partially shielded from cosmic rays by the Earth's magnetic field. Measurements in the stratosphere (ref. 6) imply significant mixing between polar and low-latitude air, showing increases in the ^{7}Be density by a factor of 2 to 5 over the equilibrium value at 31° N. In the upper atmosphere, above 120 km, the polar production rate is about a factor of 10 higher than the average rate from 0° to 30° latitude (ref. 5). Thus, complete displacement by polar air would still leave a factor of 180 unexplained.

A second possible source of increased activity is diffusion or convection of ^{7}Be from air at lower altitudes where production rates are higher due to increased atmospheric density. The onset of diffusive equilibrium, known as the turbopause, occurs between 100 and 120 km (ref. 7). Below this the atmosphere is well mixed, while above this the various components tend to diffuse independently. Because ^{7}Be is considerably lighter than the mean atmospheric molecular weight, it will tend to diffuse upward. During periods of high solar activity (ref. 8), the estimated in-situ production rate at 120 km is a factor of 300 higher than the rate at 310 km. Below 120 km production increases rapidly; at 100 km it is a factor of 7000 higher than at 310 km. Thus, the amount of diffusion will be effected by the height of the turbopause. Temperature is also an important factor. The equilibrium distribution of atmospheric molecules due to diffusion is a decreasing exponential function of the altitude with a scale height (ref. 9) which is proportional directly to the temperature and inversely to the atomic weight. The mean global temperature (ref. 10) rises rapidly from about 380K at 120 km to 1040K above 200 km. During periods of high solar activity, temperatures as high as 1700K have been measured (ref. 11,12). For ^{7}Be, this corresponds to a scale height of 206 km and an average thermal velocity of 2.5 km/s.

Several large solar flares occurred in 1989, including the late September-early October flare which was the largest in 33 years and had a very hard spectrum (ref. 13). Such events cause heating and expansion of the upper atmosphere, where winds have been measured at several hundred meters per second (ref. 11,12), driven by solar activity, diurnal solar heating and geomagnetic storms. These act both to mix polar and lower latitude air and to transport air upward from lower altitudes (ref. 9,11). The relative importance of diffusion versus convection in contributing to the increased ^{7}Be density at 310 km needs to be determined by detailed modeling of the upper atmosphere.

CONCLUSIONS AND IMPLICATIONS FOR FUTURE SPACECRAFT

Our observations of ^{7}Be activity on the leading surfaces of the LDEF spacecraft imply a minimum density for ^{7}Be in low-earth orbit which greatly exceeds the local equilibrium due to cosmic-ray production in situ. One possible explanation would require the transport by diffusion or atmospheric mixing of ^{7}Be from much lower altitudes and higher latitudes into the LDEF orbit. Thus, the current results should be important for validating and refining models of the upper atmosphere. With more extensive measurements, ^{7}Be should prove valuable as a natural tracer for studies of upper atmospheric mixing. The next step is to combine existing atmospheric circulation models with calculations of ^{7}Be production rates at lower altitudes in order to predict the upward transport of ^{7}Be. Future observations should focus on sampling at both lower and higher altitudes and should extend to polar latitudes. These should be closely correlated with data on wind, temperature, pressure and solar activity.

In addition, the observation of the accretion of significant quantities of ^{7}Be is an indication of possibly similar behavior for other light cosmic-ray produced isotopes. Table II gives the spallation yields (ref. 5) for all light isotopes with yields greater than or of the order of ^{7}Be. Also given are their halflives and decay modes. ^{3}He is stable and non-reactive. The remaining isotopes, other than ^{7}Be, are all pure beta emitters and thus would not be seen in the present survey. They could, however, be significant sources of noise for low-level sensors on spacecraft in low-earth orbit and could slowly degrade other components by coating or by surface reactions. Lithium, the decay product of ^{7}Be, could affect exposed semiconductor sensors even in very low concentrations. As a result of our observations, other groups are currently looking for trace amounts of Li, ^{14}C and ^{10}Be on LDEF components.

A period of 23 days elapsed between the time of the LDEF capture by the shuttle and the start of the gamma ray survey. Thus much of the short-lived activity had decayed away before we were able to observe it. A gamma ray survey should be made of a shuttle immediately after landing to determine the magnitude and significance of this activity.

APPENDIX

Equilibrium ^{7}Be Density from Cosmic-Ray Production

Lal and Peters (ref. 5) provide curves of cosmic-ray production rates (interactions per gram of air per second) versus latitude and altitude, using a model derived from measurements during a period of high solar activity. From these curves and the known spallation yields (ref. 5), we obtain a ^{7}Be production rate per gram of air between 0° and 30° latitude of 9.0×10^{-5} atoms/g-s at the "top" of the atmosphere (above 120 km). The mean atmospheric density during periods of high solar activity (ref. 8) at an altitude of 310 km is about 6.1×10^{-8} g/m^3. This gives an in-situ production rate for ^{7}Be at 310 km of 5.5×10^{-12} atoms/m^3-s. Multiplying by the equivalent in seconds of the 77 day mean ^{7}Be lifetime gives an equilibrium density for ^{7}Be of 3.6×10^{-5} atoms/m^3, due to production in situ.

The trapped proton flux provides an added production source of ^{7}Be at 310 km. Using the trapped proton fluence for solar maximum given by Stassinopoulos (ref. 14), the average equilibrium density of ^{7}Be is 1.8×10^{-5} atoms/m^3. Adding this to the density due to cosmic-ray production gives a total density which is then 5.4×10^{-5} atoms/m^3. However, the "average" density calculated for the trapped protons is somewhat misleading since virtually all the production occurs in the South Atlantic Anomaly where the density would be considerably higher.

Minimum ^{7}Be Density from Our Measurements

Our measurements of the ^{7}Be activity on the LDEF leading edge give an average surface density for ^{7}Be of $(5.4 \pm 1.4) \times 10^9$ atoms/m^2, corrected to the date of retrieval of the spacecraft. With an orbital velocity of 7.8 km/s, LDEF traveled a distance of 5.2×10^{10} m during one mean lifetime of ^{7}Be. Dividing the surface density by this distance gives the mean capture rate of ^{7}Be in orbit. Assuming 100% adherence of ^{7}Be to the surface of LDEF, this implies a minimum density in orbit for ^{7}Be of 0.10 ± 0.03 atoms/m^3. (Less than 100% adherence would imply an even greater ^{7}Be density in orbit.)

REFERENCES

1. G.W. Phillips and K.W. Marlow, Nucl. Instr. and Methods; vol. 137, 1976, pp. 525-536.
2. S.E. King, et al., IEEE Transactions in Nuclear Science, vol. 38, 1991, pp. 525-530.
3. J.W. Watts, T.A. Parnell, and H.H. Heckman, AIP Conference Proceedings, no. 186, High Radiation Background in Space, ed. A.C. Rester, Jr., and J.I. Trombka, AIP, New York, 1987, pp. 75-85.
4. G.J. Fishman, et al., Nature, vol. 349, 1991, pp. 678-680.

5. D. Lal and B. Peters, Encyclopedia of Physics, vol. 46/2, ed. K. Sitte, Springer, New York, 1967, pp. 551-612.
6. N. Bhandari, J. Geophys. Res., vol. 75, 1970, pp. 2927-2930.
7. I. Harris and N.W. Spencer, Introduction to Space Science, ed. W.N. Hess and G.D. Mead, Gordon and Breach, New York, 1968, pp. 93-131.
8. Appendix C, COSPAR International Reference Atmosphere: 1986, Part 1: Thermospheric Models, ed. D. Rees, Pergamon Press, New York, 1989, pp. 315-470 (see Table 5.12.)
9. J.K. Hargreaves, The Upper Atmosphere and Solar-Terrestrial Relations, Van Nostrand Reinhold, New York, 1979.
10. A.E. Hedin, COSPAR International Reference Atmosphere: 1986, Part 1: Thermosphere Models, ed. D. Rees, Pergamon Press, New York, 1989, pp. 9-25.
11. N.W. Spencer and G.R. Carignan, ibid., pp. 107-117.
12. G. Hernandez and T.L. Killeen, ibid., pp. 149-213.
13. J.H. Allen, 1989 Solar Activity and its Consequences at Earth and in Space, presented at the DOD-DOE-NASA Seventh Symposium on Single Event Effects, May 1990.
14. E.G. Stassinopoulos and J.M. Barth, Goddard Space Flight Center Report No. X-600-87-7, Greenbelt, MD, 1987.

TABLE I. - OBSERVED GAMMA-RAY ACTIVITIES ON LDEF

Isotope	γ-ray Energy	Half-Life	Activity	
	keV		10^{-3}c/s/det	% error
β^+ annih.	511	na	112.	0.8
^{22}Na	1274	2.6 y	39.7	0.3
^{7}Be*	478	53 d	23.0	3.
^{54}Mn	835	312 d	3.1	4.
^{57}Co+	122	272 d	2.8	23.
^{56}Co	847	78 d	0.75	25.
^{60}Co	1173, 1332	5.3 y	0.34	27.
* Peak activity at row 9 is given for ^{7}Be				
+ Activity for ^{57}Co is averaged over 4 rows only				

TABLE II. - COSMIC RAY PRODUCED LIGHT ISOTOPES

Isotope	Yield/Interaction	Half-Life	Decay Modes
^{14}C	1.5*	5.7 x 10^4 y	beta
^{3}H	0.14	12.3 y	beta
^{3}He	0.12	stable	none
^{7}Be	0.045	53 d	ec+, gamma
^{10}Be	0.025	1.6 x 10^6 y	beta
* Relative yield, produced mainly by thermal neutrons			
+ Electron capture, gamma branching ratio 10.4%			

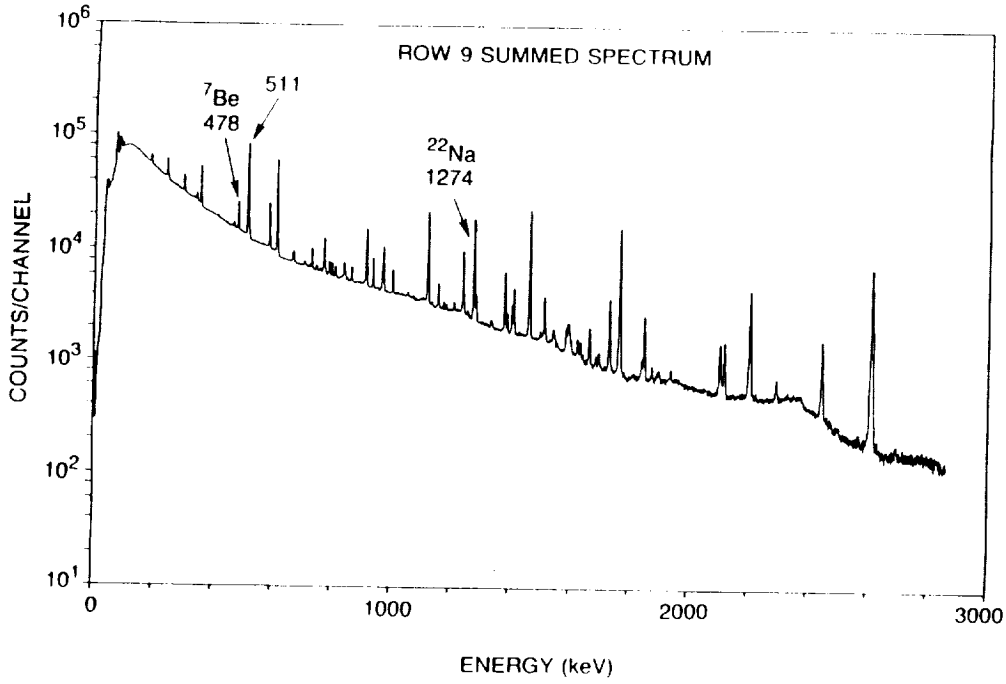

Figure 1. Summed spectrum along LDEF row 9 at the leading edge of the spacecraft. The peaks from ^{7}Be, ^{22}Na, and positron annihilation (511) are indicated. Most of the remaining prominent peaks are from the background. Accumulation time was 29 hours, and the energy calibration is 0.706 keV/channel.

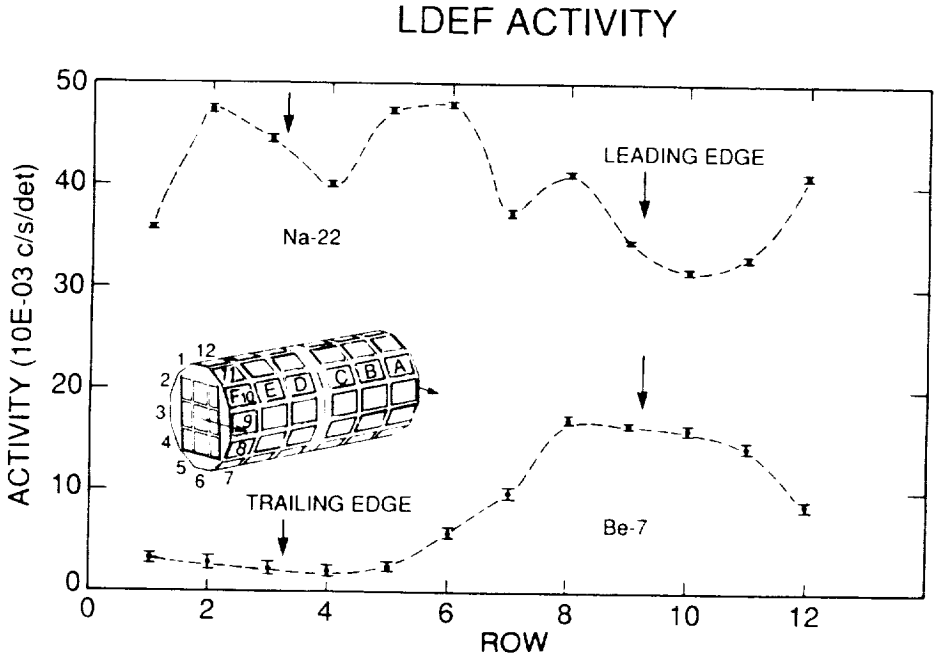

Figure 2. Comparison of activities of ^{7}Be (lower) and ^{22}Na (upper) seen during the gamma-ray survey of the LDEF spacecraft. The average counts per second per detector are shown for each row of LDEF for an average detector efficiency of 38.8% at 1332 MeV relative to a 7.6 x 7.6 cm diameter NaI(Tl) detector. The error bars include statistical and peak-fitting uncertainties. As a visual aid, dashed curves are drawn connecting the data points. The overlay is a diagram of LDEF.

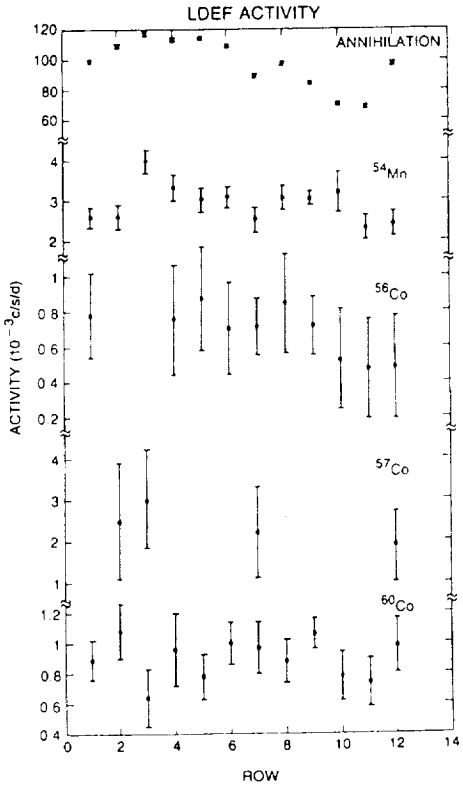

Figure 3. Distribution of activities from positron annihilation, ^{54}Mn and ^{56,57,60}Co around the LDEF spacecraft. Background activity has been subtracted. The error bars include statistical and peak-fitting uncertainties.

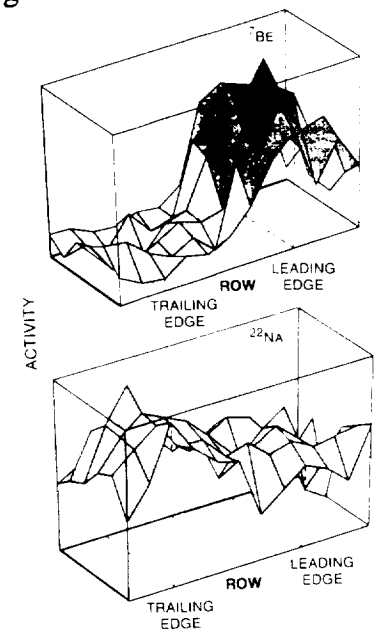

Figure 4. Map of the distribution of ^{7}Be and ^{22}Na activities around the LDEF spacecraft. There are 12 rows along the right axis and six bays along the left axis, with data from one experimental tray plotted for each bay and row. The dashed lines indicate the positions of the leading and trailing edges. The ^{7}Be activity is strongly peaked along the leading edge, while the ^{22}Na activity is higher along the trailing edge.

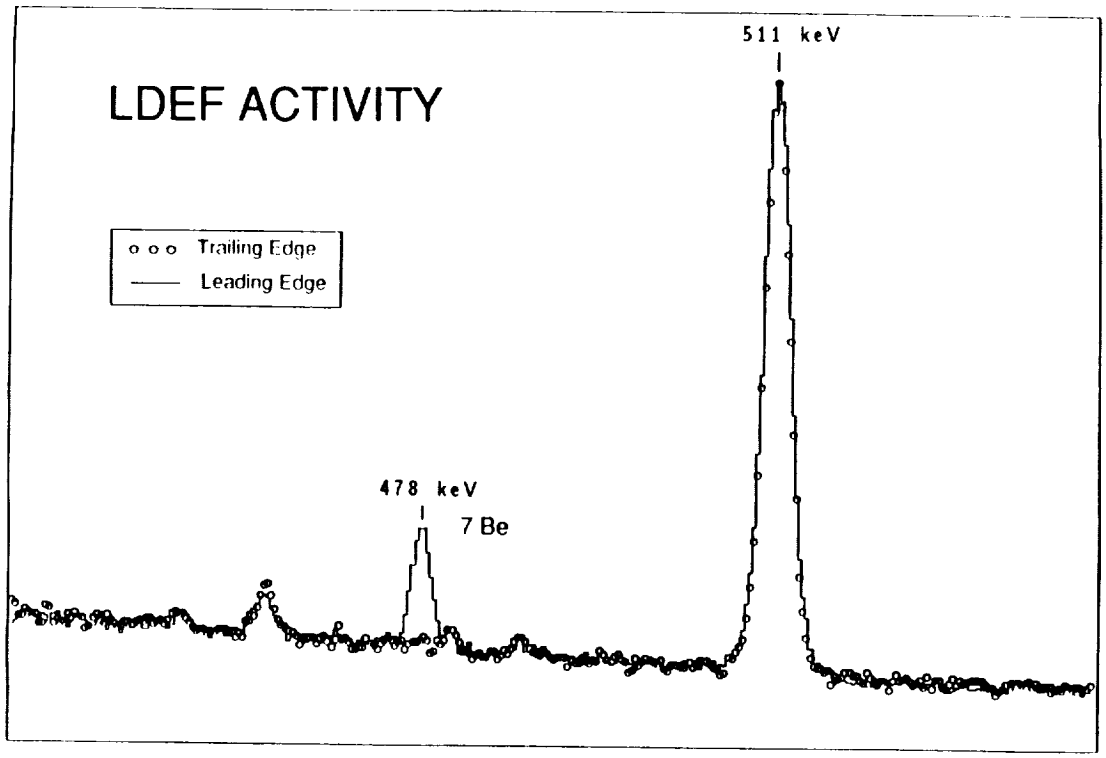

Figure 5. Comparison of gamma-ray spectra of germanium plates from trays E3 and E8 after their removal from LDEF. Shown is the region including the 478 keV gamma ray from ^{7}Be which is seen on tray E8 near the leading edge and not on tray E3 at the trailing edge. The 511 keV peak due to positron annihilation is seen both in the background and from ^{22}Na. The weaker unlabeled peaks are all in the background.